J Electroceram (2011) 26:8–13
DOI 10.1007/s10832-010-9620-9

Multiferroic ceramics $Pb(Fe_{1/2}Nb_{1/2})O_3$ doped by Li

Dariusz Bochenek · Pawel Kruk · Ryszard Skulski · Pawel Wawrzała

Received: 12 November 2008 / Accepted: 3 October 2010 / Published online: 20 October 2010

Abstract We present the results of obtaining and investigating multiferroic ceramics $Pb(Fe_{1/2}Nb_{1/2})O_3$ (PFN) and PFN doped by various amounts of Li (PFN:Li). Ceramics have been obtained from oxides by two-step synthesis. For obtained samples the X-ray diffraction patterns, microstructure, DC electric conductivity, the temperature dependencies of dielectric permittivity and dielectric losses, electromechanical properties and hysteresis loops have been investigated. Obtained results have shown that the introduction of Li decreases electric conductivity and improves dielectric and electromechanical parameters important for applications.

Keywords Intelligent materials · Multiferroics · Columbite method · PFN

1 Introduction

Intelligent materials are able to change their properties according to external factors and those changes remain after removing the factors mentioned. Materials with constant properties which do not change properties in such a way (for example: gold, silver, platinum, diamond etc.) cannot be included into the group of intelligent materials (also called smart materials). Intelligent materials have one or more properties that can be dramatically altered. There are many types of smart materials, for example piezoelectric materials, fluids changing their viscosity under magnetic or electric field (magneto-rheostatic or electro-rheostatic materials) and shape memory alloys. The special group of smart materials are ferroics and multiferroics. Ferroics are materials in which the answer of hysteretic type is related to only one precisely defined external factor. The term multiferroic was first used by H. Schmid in 1994 [1] for materials that exhibit more than one primary ferroic order parameter simultaneously with another ones. Materials with two ferroic order parameters are called biferroics. Recently, a lot of excellent theoretical and review papers have been published for example [2–6]. Materials exhibiting such activity can be used in various forms (single crystals, polycrystallic ceramic materials, composite materials, thin films, multilayer materials etc.) for construction of many units (for example artificial intelligence units [7]). Obtaining such materials requires advanced technologies.

$Pb(Fe_{1/2}Nb_{1/2})O_3$ (PFN) belongs to the biferroic materials. Undoped PFN exhibits simultaneously ferroelectric and antiferromagnetic properties below -130°C (143 K). At the temperatures range from -130°C (143 K) to +115°C (388 K) this material is a relaxor ferroelectric. This compound has been described by Smolensky [8] and Venevcev [9] in the fifties and sixties of the previous century. The structure of PFN is perovskite type. The elementary cell contains Fe^{3+} ions and Nb^{5+} in B-positions, while Pb^{2+} ion occupies A-positions [10]. According to relatively easy process of synthesis, low temperatures of sintering, low reactivity and high value of dielectric permittivity, PFN is still an attractive material for commercial electroceramics [11]. The main problem during obtaining PFN ceramics is formation of the second non-perovskite phase (pyrochlore) and related to this high dielectric losses and high dielectric conductivity. It narrows down the possibility of wide applications of this material in the electronic devices. It is possible to reduce these negative phenomena by doping PFN, for example by Li [12].

D. Bochenek · P. Kruk · R. Skulski · P. Wawrzała (✉)
Faculty of Computer Science and Materials Science,
Department of Material Science, University of Silesia,
2 Śnieżna Str.,
Sosnowiec 41-200, Poland
e-mail: pawel.wawrzala@us.edu.pl

Another possibility is appropriate and careful processing of ceramics with excess of PbO.

In this work we have developed the technology of PFN and PFN:Li. For the obtained samples we investigated the effects of lithium doping on the electrical conductivity and another basic parameters of PFN and PFN:Li ceramics. Li addition has been introduced into the PFN base in the amount of 0.5, 1.0, 1.5, 2.0% at.

2 Experimental

Ceramic samples of $PbFe_{1/2}Nb_{1/2}O_3$ have been obtained using two-step technology (called the columbite method although the columbite is $MgNbO_3$). The technological steps were as follows:

- drying and weighting the powders Fe_2O_3 and Nb_2O_5 for obtaining $FeNbO_4$ (i.e. without PbO);
- mixing the powders for 8 h (at every stage of the technology of $FeNbO_4$ and PFN);
- the synthesis of powders (calcination) in the air according to reaction: $Fe_2O_3+Nb_2O_5 \rightarrow 2FeNbO_4$ in conditions: $T_{s1}=1000°C$ and $t_{s1}=4$ h;
- weighting $FeNbO_4$, PbO and Li_2CO_3. Expecting the possible losses of the lead the 2.5% excess of PbO has been added. Lithium has been introduced as Li_2CO_3 according to reaction: $0.5FeNbO_4 + (1-x)PbO + xLi_2CO_3 \rightarrow Pb_{1-x}Li_{2x}\left(Fe_{1/2}Nb_{1/2}\right)O_3 + xCO_2 \uparrow$ with x=0.0025, 0.05, 0.075, 0.01. Samples obtained in such a way are denoted below $PL_{0.5}FN$, $PL_{1.0}FN$, $PL_{1.5}FN$ and $PL_{2.0}FN$;
- the synthesis (calcination) of such prepared powders at $T_{s2}=800°C$ and $t_{s2}=3$ h;
- pressing into pellets;
- the final sintering in alumina crucibles in air at $T_s=1050°C$ and $t_s=2$ h.

The obtained samples were discs with diameter $\varphi \approx 10$ mm and thickness $d \approx 1$ mm. Silver electrodes have been put on both sides of the samples.

The following investigations have been carried out for obtained ceramic samples:

- XRD tests of crystallographic structure using Philips X'pert diffractometer
- the microstructure investigations using SEM HITACHI S-4700 scanning microscope
- resistivity measurements in the temperature range (20–400)°C using Tesla BM518 m
- the measurements of dielectric parameters using Quad-Tech 1920 Precision LCR Meter
- electromechanical measurements using Philtec Inc. D63 and high voltage amplifier Matsusada HEOPS-5B6 controlled by PC
- the hysteresis loop investigations using the same equipment as for electromechanical measurements.

3 Results and discussion

X-ray diffraction patterns for all investigated compositions are presented in Fig. 1 (in logarithmic scale). All maxima belong to the perovskite phase, so we can conclude that the samples are single phase—perovskite (i.e. without the pyrochlore phase). At the room temperature the structure of the samples is tetragonal. It has also been observed that the introduction of Li into PFN slightly changes the elementary cell parameters (Table 1), however we did not observe any distinct relation between the amount of lithium addition and the volume of elementary cell.

The obtained material has high density (Table 1) and relatively large grains with dimensions between 3.2÷5.5 μm. On the basis of the selected SEM images of the samples fractures (Fig. 2) it can also be stated that large heterogeneity of grain sizes takes place. It is seen in Fig. 2 (a), (b) and (c) that all the grains are broken. On the other hand in case of Fig. 2(d) and e there are also seen grains which are unbroken what can be related to the fact that the strength of grain inside is higher than at the grain boundaries. So we can conclude that the introduction of lithium at the amount 1.5%at. and 2%at. improves the strength of grain

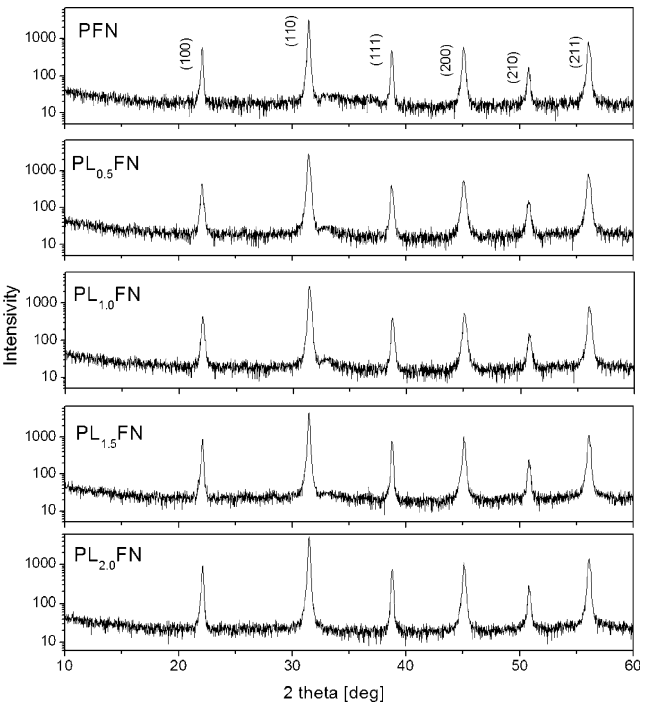

Fig. 1 X-ray diffraction patterns of PFN ceramics with various amounts of Li-addition

Table 1 The influence of the Li-addition on the PFN ceramics parameters

	PFN	$PL_{0.5}FN$	$PL_{1.0}FN$	$PL_{1.5}FN$	$PL_{2.0}FN$
Li content [at. %]	0	0.5	1.0	1.5	2.0
$\rho \cdot 10^{-3}$ [kg/m^3]	7.89	7.95	7.90	8.02	8.05
a [Å]	4.02	4.02	4.02	4.02	4.02
c [Å]	4.01	4.01	4.02	4.02	4.01
V [Å^3]	64.75	64.75	64.81	64.98	64.68
T_m [°C]	99	96	89	85	79
ε_r	3,450	2,900	2,260	2,480	2,290
ε_m	25,590	22,130	26,070	36,040	43,810
$\varepsilon_m/\varepsilon_r$	7.4	7.6	11.5	14.5	19.1
tanδ at T_r	0.181	0.011	0.033	0.017	0.026
tanδ at T_m	0.238	0.202	0.237	0.079	0.039
α	1.93	1.82	1.80	1.77	1.74
E_{a1} [eV] at I range	0.21	0.42	0.38	0.34	0.46
E_{a2} [eV] at II range	0.79	–	–	0.44	0.10
E_{a3} [eV] at III range	0.66	0.85	0.86	1.18	0.99
P_s [μC/cm^2]	20.16	17.90	17.57	21.80	24.23
P_r [μC/cm^2]	14.59	10.85	12.60	16.82	19.77
E_c [kV/mm]	0.51	0.35	0.38	0.29	0.25
S_r [%]	0.003	0.0015	0.022	0.027	0.038
H_s [%]	6.93	73.50	1.99	19.21	6.69

boundaries. The optimal shape of grains which is seen in Fig. 2(e) i.e. for $PLi_{2.0}FN$ is connected with the highest strength of grain boundaries as well as the insides.

Figure 3 shows the dependency $\ln\sigma(1/T)$ for PFN and PFN:Li. For lithium amount below 1.5%at. with increasing Li contents DC conductivity decreases. For the linear parts of $\ln\sigma(1/T)$ plots it was possible to calculate the activation energy from formula:

$$\sigma = \sigma_0 e^{-\frac{E_a}{kT}} \tag{1}$$

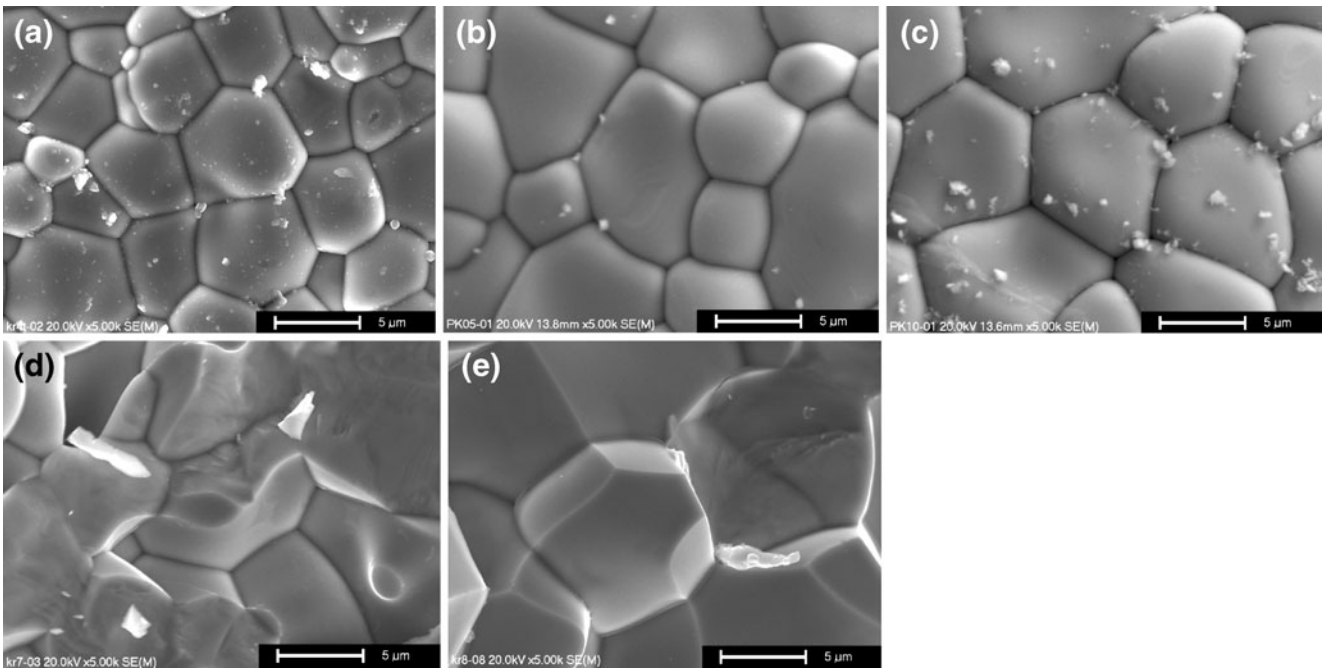

Fig. 2 The influence of Li addition into PFN ceramics on the microstructure of the samples: (**a**) PFN, (**b**) $PL_{0.5}FN$, (**c**) $PL_{1.0}FN$, (**d**) $PL_{1.5}FN$, (**e**) $PL_{2.0}FN$; scale bar 10 μm

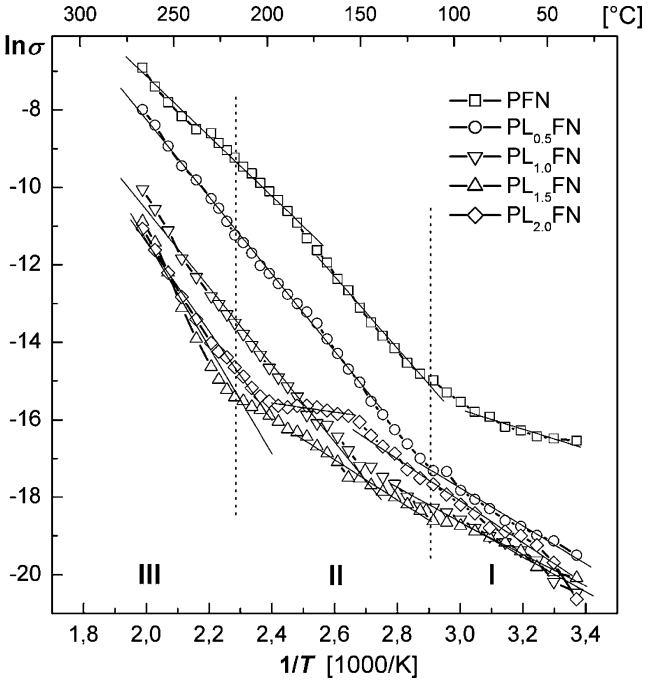

Fig. 3 The influence of Li addition into PFN ceramics on lnσ (1/T) dependencies I, II, III—indicates ranges with different activation energy, respectively E_{a1}, E_{a2}, E_{a3}—see Table 1

where: σ—conductivity at given temperature, σ_0 - pre-exponential factor, E_a - activation energy, k - Boltzman constant, T - temperature. Values of activation energy obtained in such a way (Table 1) are of the same order as for example in works [12, 13]. At the low temperatures (range I) the values of activation energy are lower than the values at the highest temperatures (range III). There are also the samples in which it was possible to distinguish three temperature ranges. Generally the higher the Li amount the higher the activation energy (Table 1). In the work of

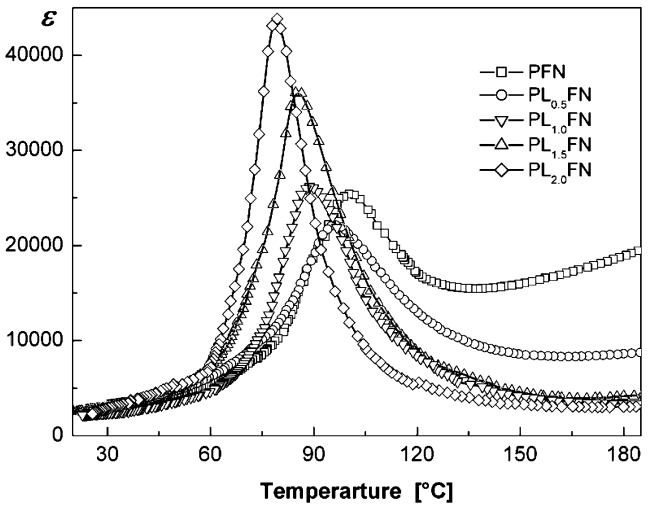

Fig. 4 Dependencies $\varepsilon(T)$ for various Li contents (ν=1 kHz)

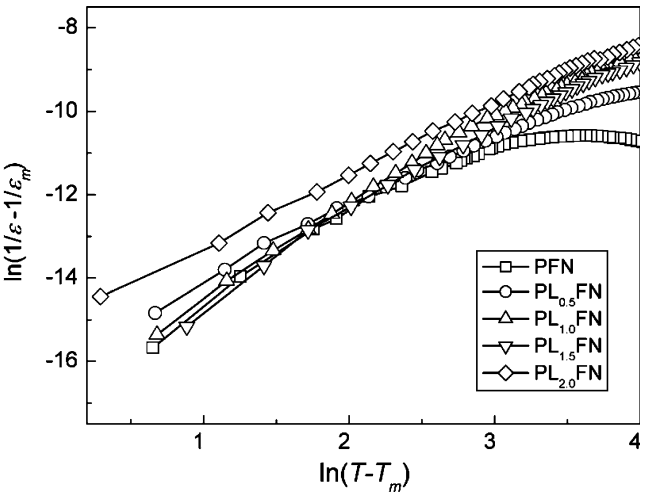

Fig. 5 Plots of ln($1/\varepsilon$-$1/\varepsilon_m$) vs. ln(T-T_m) for pure PFN ceramics and Li doped compositions (for paraelectric phase)

Zieleniec et. al. [12] the influence of the Li addition on the type of conductivity of PFN ceramics was also investigated. It has been stated that for Li amount smaller than 0.5%at. the conductivity is n-type within the temperature range 102÷452°C (375÷725 K) though the values of activation energy change in this range. For 1%at. Li the conductivity is p-type. For 2%at. Li the conductivity is change at about 297°C (570 K) from p-type to n-type (on heating).

Dependencies $\varepsilon(T)$ measured at 1 kHz are presented in Fig. 4. It is seen that with increasing Li content the maximum of dielectric permittivity increases with simultaneous shift towards lower temperatures. The highest temperature of the phase transition was observed for undoped PFN, while the lowest one for $PL_{2.0}FN$ (Fig. 4 and Table 1).

Figure 4 also shows that for all samples the phase transition is diffused although the degree of diffusion is

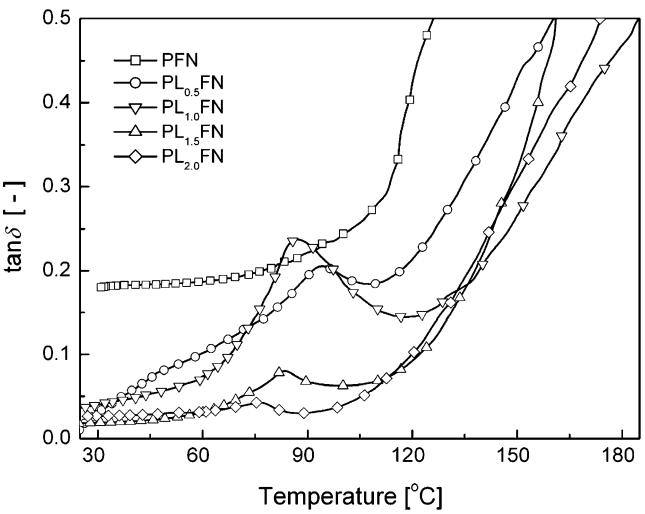

Fig. 6 The dependencies of tanδ on temperature for PFN with Li addition (ν=1 kHz)

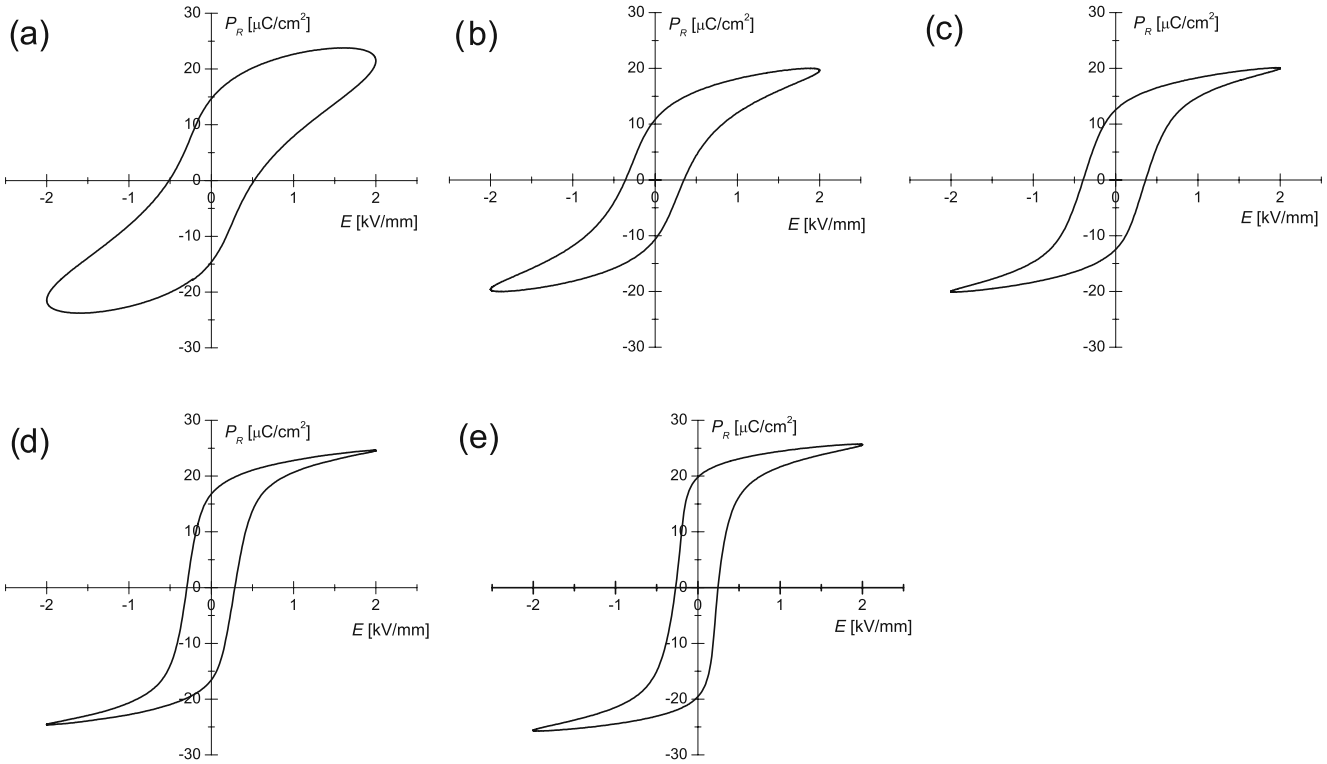

Fig. 7 P-E hysteresis loops at room temperature and frequency 1 Hz for: (**a**) PFN, (**b**) $PL_{0.5}FN$, (**c**) $PL_{1.0}FN$, (**d**) $PL_{1.5}FN$, (**e**) $PL_{2.0}FN$

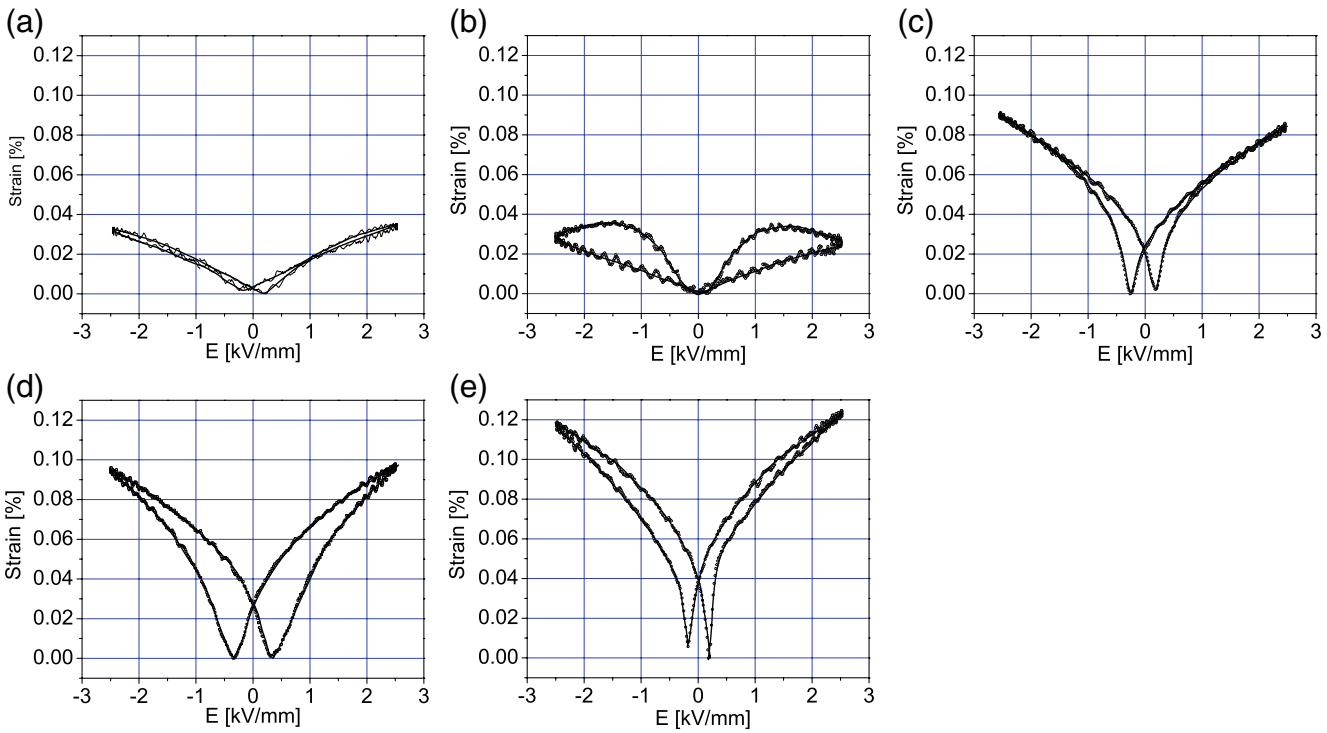

Fig. 8 Effect of Li-addition to PFN ceramics on strain-electric field loops (v=1 Hz): (**a**) PFN, (**b**) $PL_{0.5}FN$, (**c**) $PL_{1.0}FN$, (**d**) $PL_{1.5}FN$, (**e**) $PL_{2.0}FN$

different. As a measure of the phase transition diffusion the ratio between the maximum dielectric permittivity (at temperature T_m) and the dielectric permittivity at the room temperature ($\varepsilon_m/\varepsilon_r$) (see Table 1) can be taken. The degree of diffusion can be also calculated (only for paraelectric phase) from the formula:

$$\frac{1}{\varepsilon} - \frac{1}{\varepsilon_m} = C(T - T_m)^{\alpha} \quad (2)$$

where: T_m—the temperature at which dielectric permittivity riches its maximum (ε_m), ε_m—dielectric permittivity at the temperature T_m, C—temperature independent constant, α—exponent related with the degree of diffusion of the phase transition. After finding the logarithm we obtain:

$$\ln\left(\frac{1}{\varepsilon} - \frac{1}{\varepsilon_m}\right) = \ln C(T - T_m)^{\alpha} = \ln C + \alpha \ln(T - T_m) \quad (3)$$

At the case α=1 and ε_m=1 we obtain normal Curie-Weiss law, while for $1<\alpha\leq 2$ the phase transitions is diffused. Figure 5 presents the plots $\ln(1/\varepsilon\text{-}1/\varepsilon_m)$ vs. $\ln(T\text{-}T_m)$ for $T > T_m$. Fitting data to Eq. 4 we can calculate the α parameter values. Obtained results are presented in Table 1. It is seen that with increasing Li addition the diffusion of the phase transition becomes less diffused (α decreases from 1.93 for undoped PFN to 1.74 for 2%Li).

In Fig. 6 we compared the temperature dependencies of dielectric losses (tanδ) measured with the frequency 1 kHz. For undoped PFN the value of tanδ changes only in minimal degree between the room temperature and temperature about 115 C. Above temperature of phase transition tanδ increases abruptly, which is probably the result of a conductivity increase. In samples doped by Li the anomalies of tanδ are observed at temperatures below the phase transition temperature. The highest values of tanδ have been observed for undoped PFN (Table 1).

The results of *P-E* hysteresis loops investigations (i.e. polarization switching) at room temperature and the frequency 1 Hz are shown in Fig. 7. A distinct difference in the shape of hysteresis loop between undoped PFN and Li-doped samples can be observed. The loops for PFN:Li are more saturated than undoped PFN. With increasing Li-content the value of spontaneous polarization (P_s)also and remanent polarization (P_r) increase while the coercion field (E_C) decreases.

In Fig. 8 *S-E* (strain-electric field) loops for investigated samples are presented. It is seen that with increasing Li-content, the shape of *S-E* loops changes from that typical for relaxors to that typical for normal ferroelectrics. For describing of *S-E* loops shape we can use coefficient of strain H_s and the remanent strain S_r [%]. Coefficient H_s can be defined as:

$$H_S = \left(\frac{\Delta S_{half}}{S_{\max}}\right) \cdot 100\% \quad (4)$$

where: ΔS_{half}—the hysteresis of strains (i.e. the difference between maximum and minimum strain for the half of the maximum electric field [%], S_{max}—strain for the maximum electric field [%]. The obtained values are presented in Table 1. The maximum value of remanent strain S_r has been obtained for $PL_{2.0}FN$.

4 Conclusions

Above we have presented the results of investigations of PFN and PFN:Li ceramics obtained by two-step columbite method with Li-addition in amounts 0.5% at., 1.0% at.,1.5% at. and 2.0% at.

The microstructure studies have shown that the addition of lithium significantly influences the grain's sizes, shapes and properties. The best microstructure is for 2.0%at. Li.

XRD investigations have shown that the samples are single phase—perovskite (i.e. without the pyrochlore phase).

Li addition decreases the diffusion of phase transition and increases the maximum value of dielectric permittivity. The maximum of dielectric permittivity shifts towards lower temperatures. The Li-addition influences the shape of *P-E* and *S-E* hysteresis loops. With increasing lithium amount both these loops become more typical for ferroelectric materials. Other properties also become similar to normal ferroelectrics.

As a result we conclude that Li-doped PFN ceramics will be interesting materials for applications in electronic devices.

Acknowledgements Work supported by Polish Grant N N507 480237.

References

1. H. Schmid, Ferroelectrics **162**, 317 (1994)
2. S. Picozzi et al., J Phys Condens Matter **20**(43), 434208 (2008)
3. H. Schmid, J Phys Condens Matter **20**(43), 434201 (2008)
4. W. Eerenstein, N.D. Mathur, J.F. Scott, Nature **442**, 759 (2006)
5. S.W. Cheong, M. Mostovoy, Multiferroics: a magnetic twist for ferroelectricity. Nat Mater **6**, 13 (2007)
6. Z. Surowiak, D. Bochenek, J. Korzekwa, Electron Telecommunications Q **53**(2), 193 (2007)
7. Z. Surowiak, D. Bochenek, Archives of Acoustic **33**(2), 243 (2008)
8. G.A. Smoleński, W.M. Judin, Fiz. Twierdogo Tela **6**, 3668 (1964)
9. Y.E. Roginskaya, Y.N. Venevcev, S.A. Fedulov, Sov. Phys. Crystallogr. **8**, 490 (1964)
10. V.V. Bhat, K.V. Ramanujachary, S.E. Lofland, A.M. Umarli, J Magn Magn Mater **280**, 221 (2004)
11. J. Tand, M. Zhu, T. Hong, Y. Hou, H. Wang, H. Yan, Mater Chem Phys **101**, 475 (2007)
12. K. Wójcik, K. Zieleniec, M. Mulata, Ferroelectrics **289**, 107 (2003)
13. O. Raymond, R. Font, N. Juarez-Almodovar, J. Portelies, J.M. Siqueiros, J Appl Phys **97**(084107), 1–8 (2005)